UCS while drilling - actionable orebody intelligence for mining efficiency improvement.

Dr. S. Warden, Y. Solovyov, R. Griffiths,
N. Rivadeneyra, J. Minto, O. Alferez, C. Luu

January 14, 2022

Abstract

Uniaxial Compressive Strength (UCS), also known as unconfined compressive strength, is a key rock property which influences multiple steps along the mining value chain including drilling, blasting and comminution operations. UCS is usually measured on drill cores in the laboratory, a process that is both time consuming and expensive, while offering very limited sampling of the overall volume of rock to be extracted. We have developed a novel accelerometer-based measurement acquired while drilling which can determine the UCS of the rock being drilled from the vibrations induced in the drillstring. When acquired during blasthole drilling this provides high resolution UCS data with fine spatial sampling, providing a rich, statistically-significant dataset for determination of the distribution of rock strength. This information feeds into blasting and comminution optimization. Drilling through the current bench and sampling the next bench down expands the application of this measurement to drill pattern planning based on the measured mechanical properties of the next bench. RHINO™ hardware, deployment and processing is presented along with an example application to a copper porphyry mine.

1 Introduction

Measurement-While-Drilling (MWD) techniques collect drilling-related data, some of which provide insight into the drilling process and the rocks being drilled. Within the surface mining industry, these data are used to inform blast design by providing rock properties in individual blastholes (Segui and Higgins, 2002), allowing customization of explosives loading and blast patterns to local rock properties. These Drilling and Blasting (D&B) parameters influence blast fragmentation, reducing crushing and milling costs by optimizing blast comminution efficiency (Ranjbar et al. 2021). Scientometrics database analysis by Isheyskiy and Sanchidrian (2020) reveals significant growth of MWD-related references over the last 20 years, demonstrating increasing industry interest in these methods. Improvement in mine connectivity allows MWD data to be uploaded to the Cloud for subsequent processing and analysis. In addition, recent machine learning techniques help extract rock property information from MWD data (Kadkhodaie et al., 2010; Khushaba et al., 2021).

MWD parameters such as Rate of Penetration (ROP), Weight-on-Bit (WOB) and Torque-on-Bit (TOB), typically used to monitor drilling operations, can also shed light on the mechanical properties of the subsurface. However, results from this type of analysis have been mixed as the measurements are not always well calibrated and the empirical correlations observed are not universal.

One of the key mechanical properties of interest is Uniaxial Compressive Strength (UCS), which is also referred to as unconstrained compressive strength. UCS is defined as "*the maximum compressive stress that can be applied to a material, such as a rock, under given conditions, before failure occurs*" (AGI). The given conditions include single-axis compression (hence uniaxial) without perpendicular stress on the sample (hence unconstrained). UCS values typically range from less than 5MPa (very low strength or very weak rocks) to greater than 250MPa (very high strength or extremely strong rocks), as defined by the International Society for Rock Mechanics (ISRM) (Lu, 2015). UCS is typically measured in the laboratory either by a localized point load test or a larger scale compressive failure test on drilling cores collected in the field. Core collection and analysis is a time-consuming and expensive process, preventing real-time data analysis and decision making (Gao et al., 2021; Wang et al., 2020). As discussed by Wang et al. (2020) when working with fractured rocks, samples are

sometimes impossible to prepare. In addition, the limited number of samples being tested naturally leads to sparse representation of the rock volume to be mined.

Nainggolan et al. (2018) have shown a good correlation between UCS and blast outcomes as a function of powder factor (the ratio of the mass of explosives to the volume of rock being blasted) with higher powder factor required to deliver consistent fragment sizes with increasing UCS. UCS also supports rock classification (Rahman et al., 2021) and is a key parameter in the design of comminution circuit equipment such as crushers and SAG mills (Lu, 2015). Consequently, several authors have attempted to infer UCS from MWD parameters. For example, Li and Itakura (2012) found a proportional relation between UCS and drilling specific energy for drag bits. The UCS values predicted using this analytical model are in good agreement with those measured on rock cores but require carefully calibrated MWD measurements. More recently, Lakshminarayana et al. (2021) analyse how UCS is related to variations in the drill operating parameters monitored at a CNC drilling machine. They develop multiple higher order regression models to predict UCS from parameters such as thrust and torque.

We introduce a novel measurement derived from a vibrational time delay induced by the interaction of the bit with the rock during drilling. As a time-based measurement it eliminates the need for carefully calibrated load measurements such as weight and torque to be able to characterize the subsurface. The sensor consists of accelerometers mounted on the drillstring, from which raw acceleration time series are processed to derive a relative time delay. This time delay is subsequently correlated with independent UCS measurements to derive a transform to UCS. UCS derived in this manner can then be used to predict blast outcomes, as demonstrated with a case study from a copper porphyry mine. Further application to mill operations is also outlined.

2 RHINO™ measurement

The RHINO™ sensor system is mounted on the drillstring and consists of a set of accelerometers, batteries to power operations for up to two weeks, and a radio link to transmit the data to the surface system in the driller's cab where initial processing is performed before upload to the Cloud. In one configuration the sensor system is magnetically mounted with very strong neodymium magnets at the top of the string (Figure 1)

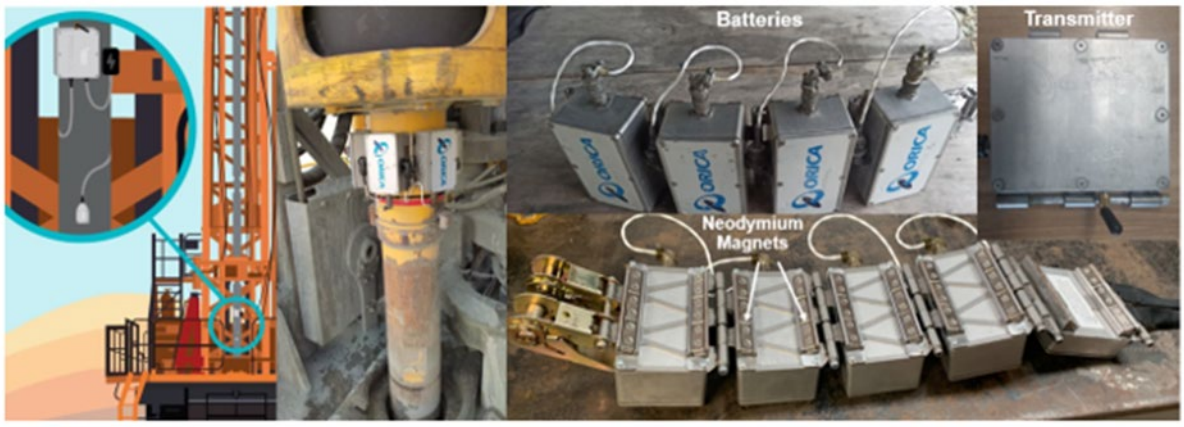

Figure 1. Sensor system deployment. Accelerometers, batteries and radio transmission modules are magnetically mounted at the top of the drillstring.

The system consists of separate radio and battery modules which can be configured to accommodate a wide range of drillstring diameters. Batteries sufficient for two weeks of continuous operation can be fitted on drill strings with a diameter of 7 5/8" or greater. Smaller drill string diameters can be accommodated but with reduced battery capacity and hence increased servicing frequency. The surface acquisition computer is connected to rig power and turns on and off with the drill rig, allowing automatic resumption of acquisition after periods of shutdown.

The radio link, used to transmit both accelerometer and system health data, can be operated across a range of frequencies around 900 MHz to comply with local regulatory or in-pit requirements. System health data such as battery voltages and Received Signal Strength Indicator (RSSI) can be monitored either locally in the driller's cab or remotely, allowing the system to be deployed on both manned and autonomous drill rigs. Data are pre-processed on the surface computer before being uploaded to the Cloud via WiFi or 4G LTE, either through the mine's network or via a third-party provider. Data are also backed up on the surface computer for subsequent manual upload in case of poor in-pit connectivity.

3 Measurement physics

During rotary drilling with a tricone bit, each bit tooth interaction with the rock behaves like a point-load UCS test as the rock is compressed until failure. As the load on the bit tooth increases the rock underneath it initially responds elastically. Obeying Newton's second law, the rock exerts a reactive force equal to the force applied by the bit during this elastic loading phase. But the reactive force is slightly time-delayed relative to the applied force as the rock deforms elastically under the bit tooth load. This delayed reactive force creates an acceleration in the drillstring which is slightly time-delayed relative to the drillstring motion that induced it (Poletto and Miranda, 2004).

Accelerometers on the drillstring measure both the original set of vibrational accelerations in the drillstring and the slightly time-delayed echo of these vibrations associated with drill bit interaction with the rock. Unlike conventional geophysical seismic measurements where the energy travels from a source to a remote receiver, this measurement utilizes the bit as both source and receiver. The near-field effects (Poletto, 2005), which result in the time delay provide a high-resolution measurement as the response occurs in the immediate proximity of the bit.

An example axial acceleration time series acquired during the drilling of a multipass hole is shown in Figure 2. Drilling took approximately 70 minutes with two rod changes at about 36 and 60 minutes after the beginning of drilling operations, as indicated by the solid black vertical lines.

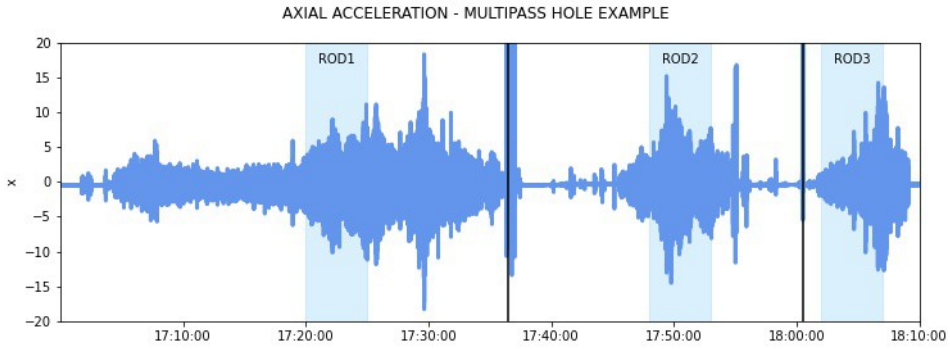

Figure 2. Example axial acceleration time series for a multipass hole. The solid vertical lines indicate the sequential addition of two rods.

The drill string has resonance frequencies at which it naturally tends to vibrate. On of the primary resonances is the axial resonance as compressional waves reflect up and down the drill string. The axial resonance frequency $f_{resonance}$ [Hz] of the system decreases as new rods are added to the drill string due to the increased length that the compressional energy must travel (Figure 3). This frequency is the inverse of the two-way travel time (TWT), where the travel time is equal to the total length of the drillstring $L_{drillstring}$ [m], divided by the group velocity V_{group} [$m.s^{-1}$]:

$$f_{resonance} = \frac{V_{group}}{2 * L_{drillstring}}$$

The group velocity is given by equation 17 in Carcione and Poletto (2001), where it is computed for the long-wavelength approximation. This expression is consistent with that of Drumheller and Knudsen (1995). The authors provide a formula for N components, which when considering a simple drillstring comprising a single pipe and a collar simplifies to:

$$V_{group} = V_p * \frac{L_{pipe} + L_{collar}}{L_{pipe}^2 + \left(\frac{A_{pipe}}{A_{collar}} + \frac{A_{collar}}{A_{pipe}}\right) * L_{pipe} * L_{collar} + L_{collar}^2)}$$

Where V_p [m.s^{-1}] is the compressional velocity in steel, L_{pipe} and L_{collar} [m] the lengths of the pipes and the collar respectively, and A_{pipe} and A_{collar} [m^2] their cross- sectional areas.

To illustrate this concept, Figure 3 displays the power spectral density for the 5 minutes intervals highlighted in light blue in Figure 2, for 1, 2 and 3 identical rods forming a drillstring; the results are shown in Figures 3 (a), (b) and (c) respectively. The dashed black lines indicate the resonance frequencies for group velocities computed using Equation 1. Even though we are using a simple model which does not account for rod thickness variations at connections, the modelled resonance frequencies match the measured frequencies closely, with the resonance frequency decreasing as new rods are added to the drillstring.

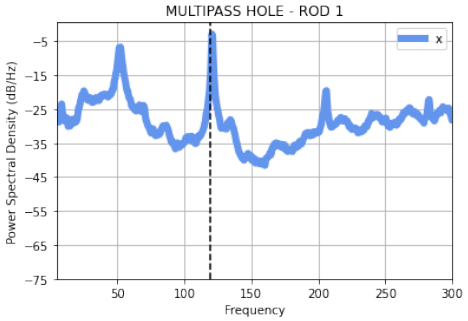

(a) 15.24 m pipe, 4.09 m collar

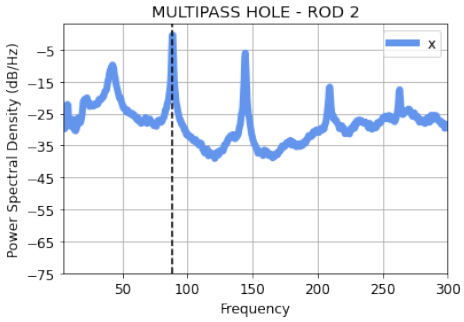

(b) 22.86 m pipe, 4.09 m collar

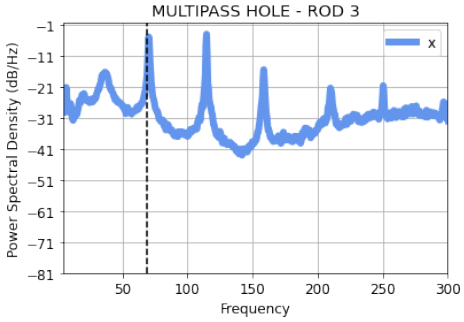

(c) 30.48 m pipe, 4.09 m collar

Figure 3. Power density spectra computed over 5-minute windows for (a) 1, (b) 2 and (c) 3 rods. The dashed black lines indicate the axial resonance frequencies computed using equation 1.

Similar analysis can be performed for the torsional, lateral and bending resonance modes of the drillstring. Knowledge of these resonance frequencies is important for the measurement as these constitute the primary vibrational modes propagating up and down the drillstring. These provide the "source signature" on which the time delay is imposed during bit interactions with the rock. Bandpass filtering is applied during processing to ensure that information imprinted on the primary resonance modes is retained while extraneous frequencies are excluded.

4 Measurement processing

One-second drillstring accelerometer traces are autocorrelated and filtered. Autocorrelation provides a relative time reference for the drillpipe acceleration waveform (Poletto and Miranda, 2004). During drilling the acceleration waveform (the vibration) in the drillpipe is continuous. The drillpipe signature reflects up and down the drillstring resulting in constructive and destructive interference with itself. There is no discrete 'source wavelet' as in conventional seismic acquisition. The slightly delayed echo of the drillpipe signature resulting from the bit interaction with the rock is extracted by filtering out the drillpipe signature while accounting for the self-interference effects. Subsequent bandpass filtering and feature extraction is used to determine the time delay.

The time delay data is time-stamped with the UTC clock time at which it was acquired. Bit depth versus UTC time information is required to allow the delay data to be plotted on a depth index. This 1D log of delay versus depth is then correlated with UCS measured on core to derive a delay to UCS transform.

5 Case Study

Data was acquired on 3 drill rigs at an open-pit copper porphyry mine over a 2-month period in late 2021. During this time 1900 blastholes were logged delivering over 33 km of data. Hole name, location and drilling depth versus time data was provided by the mine operator allowing the accelerometer data to be converted from a time-index to a 1D depth log, and it's spatial position on the bench identified. In addition, geotechnical data such as mineralogy, density, UCS and Rock Quality Designation (RQD) were provided from diamond drilled (DD) core measurements across the mine. RHINO^{TM} accelerometer measurements were acquired in 'twinned' blastholes in the immediate proximity of several of these DD holes to allow correlation of the accelerometer delay response to the core-derived measurements. UCS was measured using the point load method which involves compressing a rock sample between conical steel point load platens until failure occurs. The failure pressure is measured on a pressure gauge and is corrected to yield a point load strength index, which is then converted into a UCS value (Rusnak and Mark, 2000).

Depth adjustment of up to 1 m was required to correlate the measured delays to the core measurements. Depth uncertainties of this magnitude can be readily explained by uncertainty in depth allocation of the core depth such as due to incomplete or disturbed recovered core; discrepancies in elevation measurements of the rig while drilling the DD hole, and/or the rig while drilling the blast hole; uncertainty in the measurement of borehole inclination which results in true vertical depth uncertainty; and timing differences between the clock used to measure depth versus time, and that used to measure rock properties versus time resulting in depth uncertainty in conversion from the time- to depth-index. In addition, the while-drilling data was acquired in 'twin holes' within a meter of the core holes, but formation dip between the holes, particularly in a porphyry geological setting can be significant and abruptly changing spatially.

Figure 4 shows a cross plot of the core-derived UCS values against the measured time-delays at the corresponding depth in twin holes drilled close to the diamond drilled core holes. Fitting an exponential function to these data points provides a delay to UCS transform with a high correlation coefficient. For this configuration of the RHINO^{TM} accelerometers in this geological context the transform function was:

$$UCS = 122e^{-2.98\Delta t} \quad (3)$$

where Δt is the RHINO delay in ms.

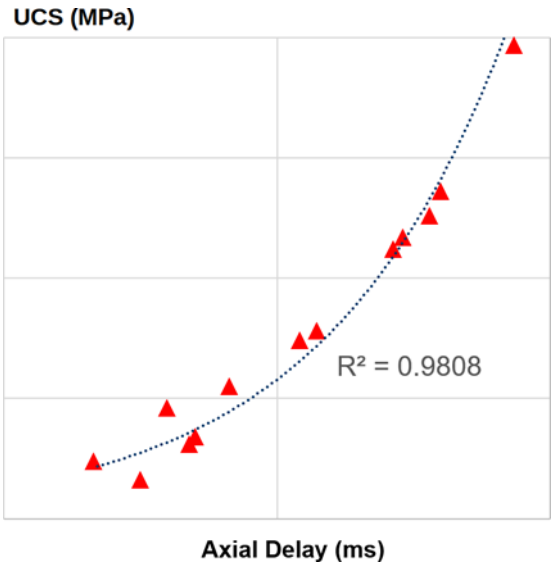

Figure 4. Cross plot of point load UCS measured on core against axial time delay measured on the accelerometers while drilling twinned blast holes in close proximity to the corresponding diamond-drilled core hole. The dotted black line shows an exponential fit with an R^2 correlation coefficient of over 0.98 demonstrating very strong correlation.

The fit is clearly better at high UCS values than at low UCS values. The authors contend that this is a result of the numerous causes that result in soft rock compared to the limited configurations that result in hard rock. For a given mineralogy, the hardest rock will tend to be homogeneous. Fracturing, weathering, porosity or any other source of heterogeneity will tend to weaken the rock. Soft rocks have a variety of mechanisms that can make them soft, not all of which will be captured during a point load test, resulting in more scatter in the point load UCS measurements for softer rocks than for the relatively homogeneous hard rocks.

Applying equation 3 to the continuous time-delay measurement acquired while drilling yields a depth-indexed log of rock UCS, an example of which is shown in Figure 5.

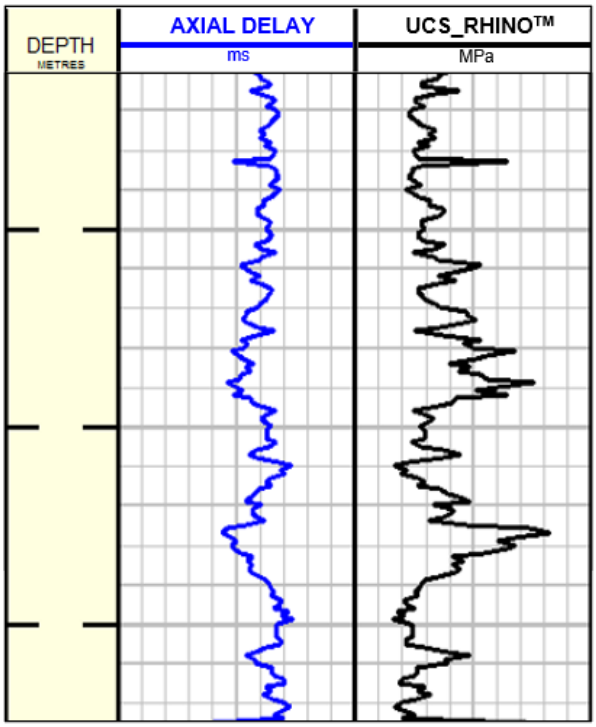

Figure 5. Depth log of measured delay time and rock UCS derived from the delay measurement,

5.1 UCS for geology

As numerous blastholes are logged across a bench, a statistically-significant sampling of the rock hardness is acquired. The distribution of rock hardness provides valuable geological information in addition to the absolute hardness of the rock. An example of this additional information is shown in Figure 6 where numerous blastholes are displayed in 3D. Colour coding shows the UCS values with blue corresponding to soft rock and red/orange corresponding to hard rock. A fault plane location (brown and blue surface) provided by the operator as part of the geological model is seen to correspond to the soft (blue) rock. This is consistent with fracturing in the proximity of the fault plane resulting in soft rock. The slight misalignment between the fault position indicated by the geological model and the soft rock as measured by the RHINO™ suggests that the geological model can be refined using the measured UCS logs.

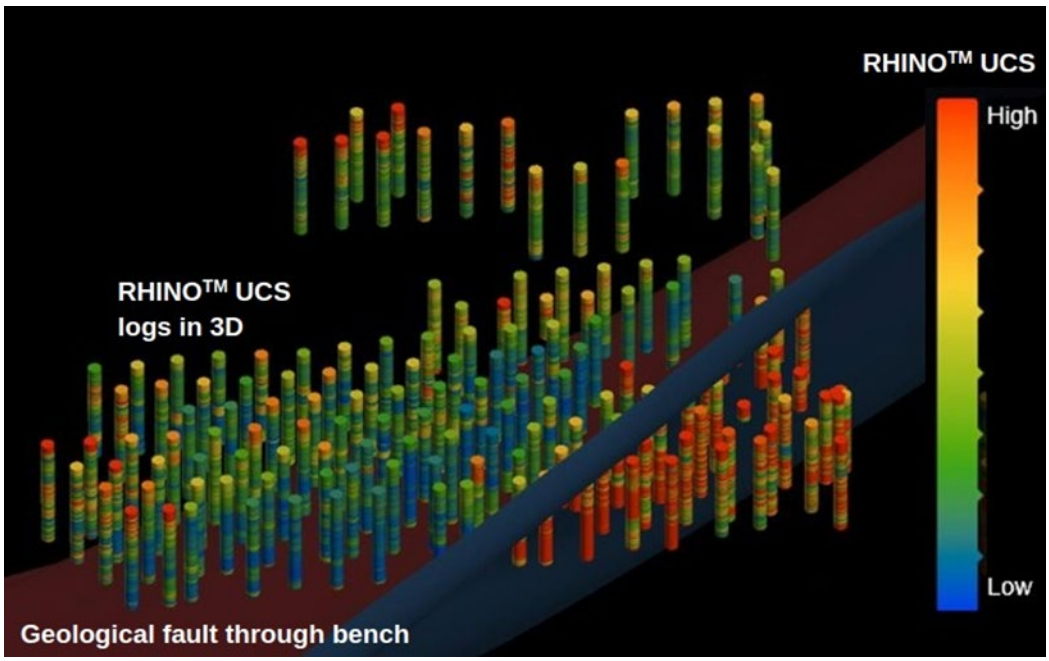

Figure 6. Aggregation of UCS data from multiple blastholes provides additional information. This 3D representation of numerous blastholes across a bench has UCS color-coded along the blastholes with high UCS values in red and orange while low UCS values appear blue and green. The low UCS (blue) interval corresponds to the location of a geological fault (brown and blue surface). The rock in this region is softer due to fracturing associated with movement of the fault. The fault location provided by the operator before drilling commenced is several meters further south than suggested by the UCS data. The availability of the array of UCS data allows the geological model to be refined.

5.2 UCS for blasting and fragmentation engineering

Where a variety of explosives are used in a single blasthole, knowledge of the UCS distribution along the blasthole allows explosives loading rules to be applied by depth. In cases where only a single explosive type is deployed in each blasthole the lateral variation of rock strength across the bench is required. Leveraging the wealth of UCS data available, a statistical analysis of the UCS distribution can be performed in each blasthole to extract the first (P25), second (median or P50) and third (P75) quartile UCS values. These can be plotted on a map allowing a simplified display of horizontal variation in rock UCS.

Figure 7 shows a colour-coded UCS map across the same drilling pattern as displayed in 3D in Figure 6. Dark colours correspond to low P75 UCS values while light colours correspond to high P75 UCS values. The dark colours correspond to the soft, fractured rock in the proximity of the fault that passes through this drilling pattern. The light colours show the harder, undisturbed rock to the south of the fault.

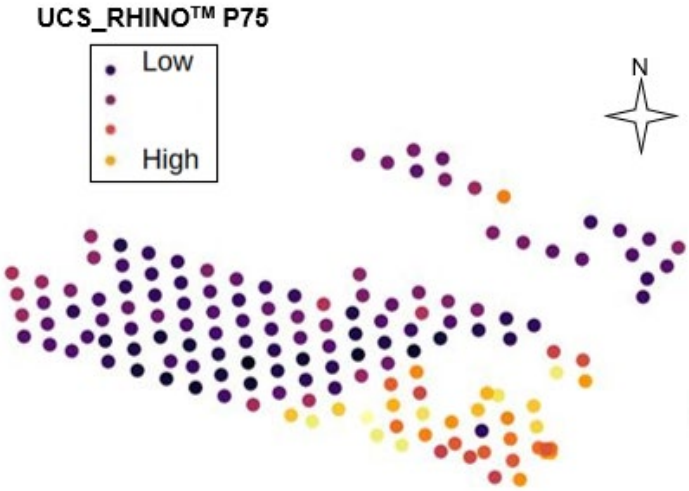

Figure 7. Horizontal variation in rock UCS value. Plotting a colour-coded map of the third quartile UCS value for each blasthole helps visualize the lateral distribution of rock hardness across a drilling pattern. This example corresponds to the pattern shown in 3D in Figure 6. Dark blue indicates low UCS rock, corresponding to the location of the fault. Lighter colours to the south of the fault indicate harder rock.

Clustering blastholes with similar rock hardness allows blasting domains to be defined. Figure 8 shows the same drill pattern presented in figure 7 clustered into four rock hardness domains. If similar fragmentation is desired across the pattern, harder zones can be loaded with higher-energy explosives while softer zones can be loaded with lower-energy explosives.

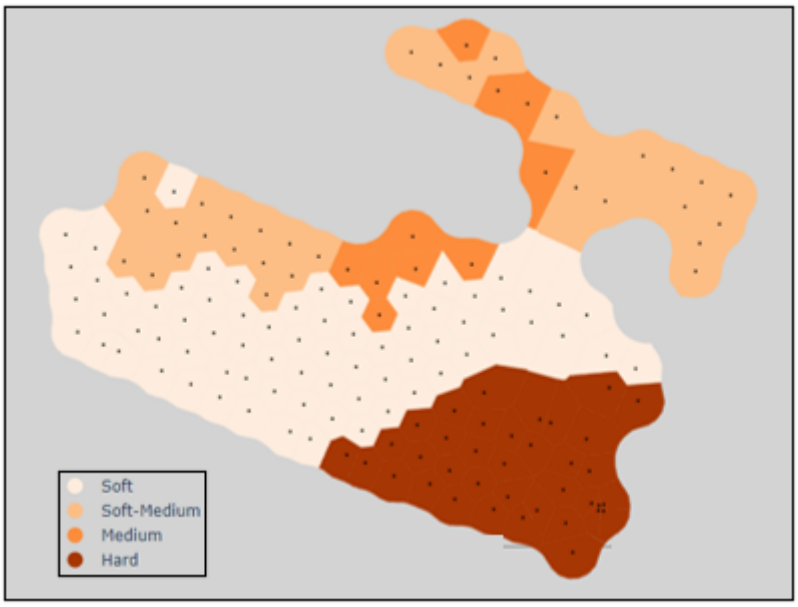

Figure 8. Blasting domains created by clustering blastholes with similar UCS values. In this example four domains have been identified. The number of domains can be adjusted according to the number of different explosive types available.

Blasting energy per unit rock mass can be changed either by changing explosive type (energy per unit explosive volume or mass) or by changing the blast hole diameter or drilling pattern (explosive volume per unit rock volume). Blasthole diameter and location cannot be changed after a blasthole has been drilled. Drilling through the current bench to sample the UCS distribution in the next bench down allows drill patterns and explosive loading plans to be formulated in advance of operations on the next bench. The detailed UCS distribution of the next bench can be assessed during blasthole drilling and explosive types/loading rules can be used to make any adjustments required to optimize rock fragmentation.

In addition to core and geological data, grade block parameters and fragmentation data were made available after blasting of blocks where RHINO™ data had been acquired. A plot of median fragment size against the median UCS measured in the corresponding grade block reveals a strong linear correlation, as shown in Figure 9. This suggests that, for a given powder factor, the median fragment size can be predicted from the median measured UCS.

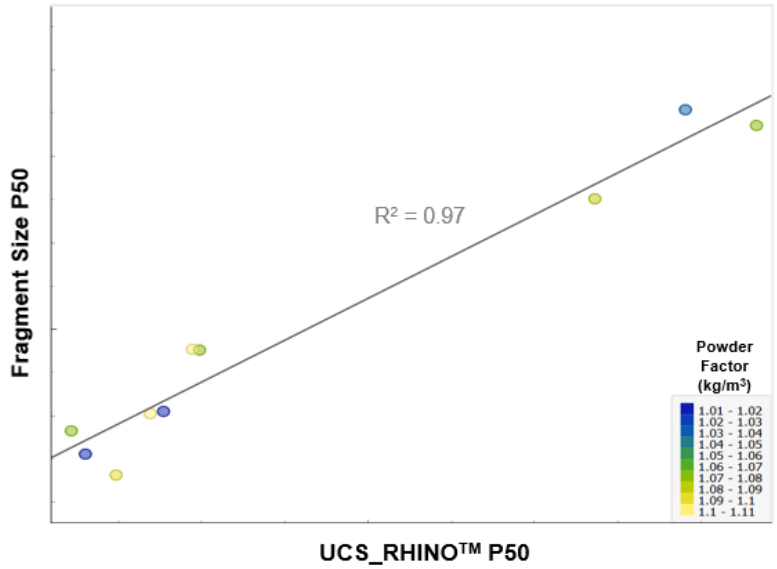

Figure 9. Fragmentation correlation to UCS for a given powder factor. The median fragment size shows a strong linear correlation to the median UCS measured in ten grade blocks that were blasted with similar powder factors.

Similar correlation with blast outcomes was performed on a number of parameters including grade block density, RQD (a rock in-situ fragmentation index), grade block UCS and median drilling rate of penetration (ROP_P50). Table 1 shows the R^2 correlation coefficients between the P20, P50 and P80 fragment sizes (mm) and the percentage of fragments less than 25 mm and 100 mm in size, against these grade block parameters. For this mine, median ROP, density and RQD (a rock in-situ fragmentation index) are poor predictors of blasting fragmentation outcome. The assigned grade block UCS is a reasonable indicator despite being sparsely sampled. The excellent correlation between UCS_RHINO™_P50 and blast outcomes appears to be a consequence of this metric capturing rock properties of direct relevance to blast outcomes (UCS) in a statistically meaningful manner by sampling the full grade block in 3-dimensions.

	Density	RQD	Grade Block UCS	ROP_P50	UCS_RHINO™_P50
P20*	0.50	0.65	0.88	0.17	0.96
P50*	0.51	0.68	0.87	0.15	0.97
P80*	0.46	0.76	0.81	0.12	0.95
25mm*	0.44	0.64	0.80	0.12	0.89
100mm*	0.46	0.75	0.79	0.09	0.94

* For grade blocks blasted with Powder Factors of 1 to 1.1 kg/m³

Table 1. R^2 correlation coefficients between measured parameters (columns) and blast outcomes (rows) for the 10 grade blocks in which the powder factor applied during blasting was between 1 and 1.1 kg/m³.

5.2 UCS for comminution circuit design

Downstream of drill and blast operations, the availability of a statistically meaningful UCS distribution of the mined ore provides opportunities to enhance stockpile management in addition to crusher and mill operations. Drop Weight Index (DWi) is a key parameter in comminution circuit design and optimization, describing the energy per unit volume required to achieve certain fragment size reduction (Morell, 2006).

The DWi has the units of kWh/m3, which is the same dimensions as strength (eg MPa) and hence it is not surprising that the DWi is correlated with direct strength measurements such as UCS. Figure 10 shows the correlation observed for point load UCS versus DWi from a DD core in the mine of interest. This clearly demonstrates that UCS is related to parameters of interest for mill performance, opening the possibility of using the measured UCS data for comminution improvement in addition to blasting optimization.

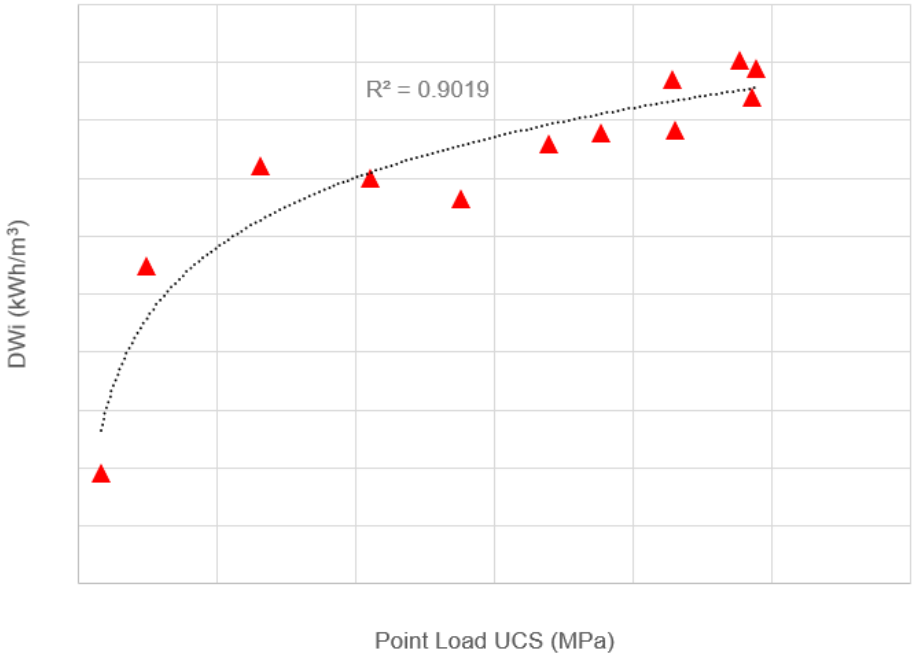

Figure 10. Drop Weight Index versus UCS showing a logarithmic correlation.

6 Conclusion

A novel accelerometer-derived measurement has been introduced which provides continuous rock UCS data while drilling. When acquired in blastholes across a bench the statistically-significant, spatially-distributed sampling of the rock UCS has been shown to correlate strongly with blast fragment size distribution. This provides the ability to predict blast outcomes and hence optimize explosives loading to deliver engineered fragmentation from blasting. UCS has also been shown to correlate with DWi, a parameter used in mill design and optimization. Hence, UCS measured while drilling provides an opportunity to enhance efficiency at various points along the mine to mill value chain.

7 References

M. Asgharzadeh, A. Grant, A. B´ona, and M. Urosevic. Drill bit noise imaging without pilot trace, a near-surface interferometry example. Solid Earth, 10:1015–1023, 07 2019. doi: 10.5194/se-10-1015-2019.

J. Carcione and F. Poletto. 2001, On the group velocity of guided waves in drill strings, j. acoust. soc. am., 109(4), 1743-1746. 01 2001.

D. S. Drumheller and S. D. Knudsen. The propagation of sound waves in drill strings. Journal of the Acoustical Society of America; (United States), 4 1995. ISSN 0001-4966. doi: 10.1121/1.412004. URL https://www.osti.gov/biblio/6488559.

A. Egorov, P. Golikov, I. Silvestrov, A. Bakulin, F. Poletto, and B. Farina. Measuring and modeling drillstring vibrations with top drive and near-bit sensors, pages 2749–2753. 2020. doi:10.1190/segam2020-3423747.1. URL https://library.seg.org/doi/abs/10.1190/segam2020-3423747.1.

D. Entwisle, P. Hobbs, L. Jones, D. Gunn, and M. Raines. The relationships between effective porosity, uniaxial compressive strength and sonic velocity of intact borrowdale volcanic group core samples from sellafield. Geotechnical and Geological Engineering, 23:793–809, 11 2005. doi: 10.1007/s10706-004-2143-x.

H. Gao, Q. Wang, B. Jiang, P. Zhang, Z. Jiang, and Y. Wang. Relationship between rock uniaxial compressive strength and digital core drilling parameters and its forecast method. International Journal of Coal Science and Technology, 8, 01 2021. doi: 10.1007/s40789-020-00383-4.

A. B. Haase and R. R. Stewart. Modelling near-field effects in vsp-based q-estimation. art. cp-40-00222, 2008. ISSN 2214-4609. doi: https://doi.org/10.3997/2214-4609.20147762. URL https://www.earthdoc.org/content/papers/10.3997/2214-4609.20147762.

V. Isheyskiy and J. A. Sanchidri´an. Prospects of applying MWD Technology for Quality Management of Drilling and Blasting Operations at Mining Enterprises. Minerals, 10(10), 2020. ISSN 2075-163X. doi: 10.3390/min10100925. URL https://www.mdpi.com/2075-163X/10/10/925.

A. Kadkhodaie, S. Monteiro, F. Ramos, and P. Hatherly. Rock recognition from mwd data: A comparative study of boosting, neural networks, and fuzzy logic. Geoscience and Remote Sensing Letters, IEEE, 7:680 – 684, 11 2010. doi: 10.1109/LGRS.2010.2046312.

R. N. Khushaba, A. Melkumyan, and A. J. Hill. A machine learning approach for material type logging and chemical assaying from autonomous measure-while-drilling (mwd) data. Mathematical Geosciences, pages 1 – 31, 2021.

C. Lakshminarayana, A. Tripathi, and S. Pal. Experimental investigation on potential use of drilling parameters to quantify rock strength. International Journal of Geo- Engineering, 12, 12 2021. doi: 10.1186/s40703-021-00152-5.

L. Li, Y. Liu, W. Liu, X. Zhang, J. Chen, D. Jiang, and J. Fan. Crack evolution and failure modes of shale containing a pre-existing fissure under compression. ACS Omega, 6(39):25461–25475, 2021. doi: 10.1021/acsomega.1c03431. URL https://doi.org/10.1021/acsomega.1c03431.

Z. Li and K. Itakura. An analytical drilling model of drag bits for evaluation of rock strength. Soils and Foundations, 52(2):216–227, 2012. ISSN 0038-0806. doi: https://doi.org/10.1016/j.sandf.2012.02.002. URL https://www.sciencedirect.com/science/article/pii/S0038080612000303.

L. Lu. Iron Ore: Mineralogy, Processing and Environmental Sustainability. Elsevier Science, 2015. ISBN 9781782421566. URL https://books.google.fr/books?id=JvkDwgEACAAJ.

S. Morrell, Design of AG/SAG Mill Circuits using the SMC test, SAG 2006

D. Nainggolan, R. Sitorus, O. Eveny, and F. Sariandi. Correlation between uniaxial compressive strength (ucs) and blasting geometry on rock excavation at pt agincourt resources. IOP Conference Series: Earth and Environmental Science, 212:012065, 12 2018. doi: 10.1088/1755-1315/212/1/012065.

F. Poletto. Energy balance of a drill-bit seismic source, part 1: Rotary energy and radiation properties. GEOPHYSICS, 70(2):T13–T28, 2005. doi: 10.1190/1.1897038. URL https://doi.org/10.1190/1.1897038.

F. Poletto and F. Miranda. Seismic While Drilling: Fundamentals of Drill-Bit Seismic for Exploration. Handbook of Geophysical Exploration: Seismic Exploration. Elsevier Science, 2004. ISBN 9780080474342. URL https://books.google.fr/books?id=HAIZdfDXT2IC.

F. Poletto, F. Miranda, B. Farina, and A. Schleifer. Seismic-while-drilling drill-bit source by ground force: Concept and application. GEOPHYSICS, 85:1–50, 02 2020. doi: 10.1190/geo2019-0449.1.

H. Rafezi and F. Hassani. Drilling signals analysis for tricone bit condition monitoring. International journal of mining science and technology, 31:187–195, 2021.

A. Ranjbar, A. Mousavi, O. Asghari, Using Rock Geomechanical Characteristics to Estimate Bond Work Index for Mining Production Blocks, Mining, Metallurgy & Exploration (2021) 38:2569–2583, https://doi.org/10.1007/s42461-021-00498-5

J. Rusnak and C. Mark. Using the point load test to determine the uniaxial compressive strength of coal measure rock. 01 2000.

J. Segui and M. Higgins. Blast Design Using Measurement While Drilling Parameters. Fragblast, 6(3-4):287–299,2002. doi: 10.1076/frag.6.3.287.14052. URL https://www.tandfonline.com/doi/abs/10.1076/frag.6.3.287.14052.

M. Wang, W. Wan, and Y. Zhao. Prediction of the uniaxial compressive strength of rocks from simple index tests using a random forest predictive model. Comptes Rendus. Mecanique, 348:3–32, 01 2020. doi: 10.5802/crmeca.3.